Vehicle tyre and handling model identification using an extended Kalman filter

Vehicle Tyre and Handling Model Identification using an Extended Kalman Filter

Matthew C Best, Andrew P Newton (Loughborough University, UK)

Dept Aeronautical and Automotive Engineering
Loughborough University, Leicestershire, LE11 3TU, UK
Phone: +44 1509 227209
Fax: +44 1509 227275
E-mail M.C.Best@lboro.ac.uk

This paper uses an Extended Kalman filter in an unusual way to identify a vehicle handling model and its associated tyre model. The method can be applied as an off-line batch process, or in real-time; here we concentrate on batch analysis of data from a Jaguar XJ test vehicle. The Identifying Extended Kalman Filter (IEKF) uses the full state measurement that is available from combination GPS / inertia instrumentation packs. Previous IEKF studies have shown success in identifying a bicycle model with a tyre force function for each axle. This paper extends to identification of a single, load dependent tyre model which applies to all four wheelstations, identified within a yaw-roll-sideslip model structure. The resulting model provides impressive open-loop state replication, including accurate tyre slip prediction across the fully nonlinear slip range of the tyre.

Topics/ 25 Modelling and Simulation Technology, 2 Tire Property, 6 Vehicle Control

1. INTRODUCTION

Within the field of chassis control, the Kalman filter is now recognised as an effective tool for observing the dynamic states of a system, and several publications describe filters for vehicle ride and handling control. In its traditional form it uses a simplified vehicle model, along with available sensor measurements, and effectively supplements the sensor information with predictions of state and sensor propagation using the model.

Clearly the accuracy of the model within the Kalman filter will greatly influence its results, so a natural goal is to maximise this accuracy. Ever increasing computing power makes more complex models viable, but with complexity comes an increase in the parameter set which needs to match the host vehicle. Moreover, if we consider how complex a model *needs* to be to achieve high accuracy, it turns out that simple models can be highly effective, provided their parameters are chosen correctly.

System identification provides a way of optimising parameters within a simple model structure and this paper explores a recent variant of the Kalman Filter, the Identifying Extended Kalman Filter (IEKF) to achieve this. Introduced in Best [1] and Best et al [2], the IEKF uses full state feedback to identify the model. The drawback is that lateral velocity is required within the vehicle's sensor set, but this is increasingly feasible given the recent development of GPS / inertia combination instrumentation sets. As it retains an iterative filter structure, the IEKF can also be used to adapt parameters in real-time, and its structure is also similar to combination state / parameter estimators such as those suggested in Bolzern et al [3] and Best et al [4].

The previous studies [1] and [2] showed that bicycle model parameters could be identified by the IEKF along with a simple Pacejka force curve describing the nonlinear force / slip behaviour aggregated at each axle. In this paper we take the model complexity slightly further in order to identify a single, nondimensional, load dependent (similarity) tyre model, in the style of that by Hugo Radt in Milliken and Milliken [5]. The nondimensional similarity model typically requires off-vehicle tyre testing, so obvious advantages exist if a similar single function for each wheelstation can be found via whole vehicle testing.

A 3dof yaw-roll-sideslip model structure is employed, because this allows more physically correct load transfer calculations than the bicycle model. The inclusion of roll also makes the resulting model more widely applicable, for example in control applications which employ suspension actuators. The required increase in complexity of the model is minimal.

The study considers test vehicle data only, and the objectives are twofold; a) to establish the feasibility of direct identification of a single uniform tyre model, and b) to show that, if appropriate parameters are optimised by system identification, the simple model structure can very accurately represent vehicle handling dynamic behaviour.

2. THE IDENTIFYING EXTENDED KALMAN FILTER (IEKF)

The standard Extended Kalman Filter (EKF) operates on nonlinear system and sensor models **f** and **h**,

which relate the true state vector $\bar{\mathbf{x}}$, measured sensor set **y**, known inputs **u** and model parameters $\boldsymbol{\theta}$ at any instant k according to

$$\dot{\bar{\mathbf{x}}}_k = \mathbf{f}\left(\bar{\mathbf{x}}_k, \mathbf{u}_k, \boldsymbol{\theta}_k\right) + \boldsymbol{\omega}_k \quad (1)$$

$$\mathbf{y}_k = \mathbf{h}\left(\bar{\mathbf{x}}_k, \mathbf{u}_k, \boldsymbol{\theta}_k\right) + \boldsymbol{\upsilon}_k \quad (2)$$

$\boldsymbol{\omega}$ thus describes the state propagation modelling error, and $\boldsymbol{\upsilon}$ gives the sensor error. $\boldsymbol{\upsilon}$ is often misleadingly referred to as the measurement error, when in reality it aggregates measurement noise within **y**, and sensor modelling errors in **h**.

An optimal filter can be derived if the error sequences obey the following

$$E\left(\boldsymbol{\omega}_k\right) = \mathbf{0}, \qquad E\left(\boldsymbol{\upsilon}_k\right) = \mathbf{0}, \qquad \forall k \quad (3)$$

$$E\left(\boldsymbol{\omega}_i \boldsymbol{\omega}_j^T\right) = \mathbf{0}, \qquad E\left(\boldsymbol{\upsilon}_i \boldsymbol{\upsilon}_j^T\right) = \mathbf{0}, \qquad \forall (i \neq j) \quad (4)$$

$$\mathbf{Q}_k = E\left(\boldsymbol{\omega}_k \boldsymbol{\omega}_k^T\right), \ \mathbf{S}_k = E\left(\boldsymbol{\omega}_k \boldsymbol{\upsilon}_k^T\right) = \mathbf{0}, \ \mathbf{R}_k = E\left(\boldsymbol{\upsilon}_k \boldsymbol{\upsilon}_k^T\right) \quad (5)$$

where the error covariance matrices $\mathbf{Q}_k$, $\mathbf{R}_k$ and $\mathbf{S}_k$ are assumed known. In practice these are difficult to estimate and they are often assumed to be time-invariant, and are also approximated, or even set nominally, with **S** often neglected as approximately zero.

The EKF also requires model Jacobians to be evaluated at each time step, defined

$$\mathbf{F}\left(\hat{\mathbf{x}}_k\right) = \left.\frac{\partial \mathbf{f}\left(\mathbf{x}, \mathbf{u}_k, \boldsymbol{\theta}_k\right)}{\partial \mathbf{x}}\right|_{\mathbf{x}=\hat{\mathbf{x}}_k}$$
$$\mathbf{H}\left(\hat{\mathbf{x}}_k\right) = \left.\frac{\partial \mathbf{h}\left(\mathbf{x}, \mathbf{u}_k, \boldsymbol{\theta}_k\right)}{\partial \mathbf{x}}\right|_{\mathbf{x}=\hat{\mathbf{x}}_k} \quad (6)$$

and the full set of equations for the standard, real-time state estimation application are

$$\mathbf{F}_k^* = \mathbf{F}\left(\hat{\mathbf{x}}_k\right) - \mathbf{S}\mathbf{R}^{-1}\mathbf{H}\left(\hat{\mathbf{x}}_k\right) \quad (7)$$

$$\mathbf{K}_k = \mathbf{P}_k \mathbf{H}^{\mathrm{T}}\left(\hat{\mathbf{x}}_k\right)\left[\mathbf{H}\left(\hat{\mathbf{x}}_k\right)\mathbf{P}_k \mathbf{H}^{\mathrm{T}}\left(\hat{\mathbf{x}}_k\right) + \mathbf{R}\right]^{-1} \quad (8)$$

$$\mathbf{P}_k^* = \left[\mathbf{I} - \mathbf{K}_k \mathbf{H}\left(\hat{\mathbf{x}}_k\right)\right]\mathbf{P}_k \quad (9)$$

$$\mathbf{P}_{k+1} = \mathbf{P}_k^* + T\left[\mathbf{Q} - \mathbf{S}\mathbf{R}^{-1}\mathbf{S}^{\mathrm{T}} + \mathbf{F}^*\left(\hat{\mathbf{x}}_k\right)\mathbf{P}_k^* + \mathbf{P}_k^*\mathbf{F}^{*\mathrm{T}}\left(\hat{\mathbf{x}}_k\right)\right] \quad (10)$$

$$\hat{\mathbf{x}}_{k+1} = \hat{\mathbf{x}}_k + \quad \cdots \quad (11)$$
$$\mathbf{K}_k\left(\mathbf{y}_k - \mathbf{h}\left(\hat{\mathbf{x}}_k\right)\right) + T\left[\mathbf{f}\left(\hat{\mathbf{x}}_k\right) + \mathbf{S}\mathbf{R}^{-1}\left(\mathbf{y}_k - \mathbf{h}\left(\hat{\mathbf{x}}_k\right)\right)\right]$$

where the filter sample time T is used to provide a simple Euler integration of the state derivatives.

Now the premise adopted in [3] and [4] is that an EKF can have its state vector augmented to include a subset of the model parameters. The resulting filter assumes no known model for the parameter variation, and simply ensures slow adaptation by adjusting the expectation of errors related to the parameter changes; so eqn (1) becomes

$$\dot{\bar{\mathbf{z}}}_k = \begin{bmatrix} \dot{\bar{\mathbf{x}}}_k \\ \dot{\bar{\boldsymbol{\theta}}} \end{bmatrix} = \begin{bmatrix} \mathbf{f}\left(\mathbf{x}_k, \mathbf{u}_k, \boldsymbol{\theta}_k\right) \\ \mathbf{0} \end{bmatrix} + \begin{bmatrix} \boldsymbol{\omega}_k^{(\mathbf{x})} \\ \boldsymbol{\omega}_k^{(\boldsymbol{\theta})} \end{bmatrix} \quad (12)$$

and the covariance $E\left(\boldsymbol{\omega}_k^{(\boldsymbol{\theta})} \boldsymbol{\omega}_k^{(\boldsymbol{\theta})T}\right)$ is then set as a tuning parameter, to adjust the rate of adaptation, ensuring this is 'slow' compared to the state propagation dynamics. This method of combining state and parameter identification is attractive, and has been shown to be effective – there is just some concern about limitations due to the combination of fast and slow dynamic responses, and the setting of error covariances.

The new identifying Kalman filter IEKF was first introduced using a simulation study in [1] and then validated using vehicle test data in [2]. It takes the parameter role one step further, for circumstances where all of the state variables are measurable. Provided $\mathbf{x}_k \in \mathbf{y}_k$ we can now form the state vector entirely as the set of parameters, such that eqns (1) and (2) become

$$\dot{\boldsymbol{\theta}}_k = \boldsymbol{\omega}_k \quad (13)$$

$$\mathbf{y}_k = \mathbf{h}\left(\mathbf{y}_{k-1}, \mathbf{u}_{k-1}, \boldsymbol{\theta}_{k-1}\right) + \boldsymbol{\upsilon}_k \quad (14)$$

The sensor equation is simply modified to include an Euler integrated propagation of each variable over a time step, to avoid identity equations. This reduces the system such that the entire model is represented within **h** alone. More importantly, it also reduces the system to a form where the error covariance matrices can be determined from the noise sequences $\boldsymbol{\omega}_k$ and $\boldsymbol{\upsilon}_k$, which are now directly calculable. The form of eqns (1) and (2) depends on the unknown $\bar{\mathbf{x}}_k$, so the error covariances cannot be explicitly determined within that filter – hence in other Kalman filter applications, **Q**, **R** and **S** are design matrices, the choice of which strongly influences the success of the resulting filter.

The IEKF propagates its own error covariances, so $\mathbf{Q}_k$, $\mathbf{R}_k$ and $\mathbf{S}_k$ are now time varying. Applying eqns (13) and (14) to the EKF formulae of eqns (7) – (11), and noting that now $\mathbf{f} = \mathbf{0}$ and $\mathbf{F} = \mathbf{0}$, we have

$$\mathbf{H}\left(\hat{\boldsymbol{\theta}}_k\right) = \left.\frac{\partial \mathbf{h}\left(\mathbf{x}_k, \mathbf{u}_k, \boldsymbol{\theta}\right)}{\partial \boldsymbol{\theta}}\right|_{\boldsymbol{\theta}=\hat{\boldsymbol{\theta}}_k} \quad (15)$$

$$\mathbf{K}_k = \mathbf{P}_k \mathbf{H}^{\mathrm{T}}\left(\hat{\boldsymbol{\theta}}_k\right)\left[\mathbf{H}\left(\hat{\boldsymbol{\theta}}_k\right)\mathbf{P}_k \mathbf{H}^{\mathrm{T}}\left(\hat{\boldsymbol{\theta}}_k\right) + \mathbf{R}_k\right]^{-1} \quad (16)$$

$$\mathbf{P}_k^* = \left[\mathbf{I} - \mathbf{K}_k \mathbf{H}\left(\hat{\boldsymbol{\theta}}_k\right)\right]\mathbf{P}_k \quad (17)$$

$$\mathbf{P}_{k+1} = \mathbf{P}_k^* + \quad \cdots \quad (18)$$
$$T\left[\mathbf{Q}_k - \mathbf{S}_k \mathbf{R}_k^{-1}\mathbf{S}_k^T - \mathbf{S}_k \mathbf{R}_k^{-1}\mathbf{H}\left(\hat{\boldsymbol{\theta}}_k\right)\mathbf{P}_k^* + \mathbf{P}_k^*\mathbf{H}\left(\hat{\boldsymbol{\theta}}_k\right)\mathbf{R}_k^{-1}\mathbf{S}_k^T\right]$$

$$\hat{\boldsymbol{\theta}}_{k+1} = \hat{\boldsymbol{\theta}}_k + \left(\mathbf{K}_k + T\mathbf{S}_k \mathbf{R}_k^{-1}\right)\left(\mathbf{y}_k - \mathbf{h}\left(\mathbf{y}_k, \mathbf{u}_k, \hat{\boldsymbol{\theta}}_k\right)\right) \quad (19)$$

where,

$$\mathbf{Q}_{k+1} = (1-\gamma)\mathbf{Q}_k + \gamma\lambda^2 \boldsymbol{\omega}_k \boldsymbol{\omega}_k^T \quad (20)$$

$$\mathbf{S}_{k+1} = (1-\gamma)\mathbf{S}_k + \gamma\lambda \boldsymbol{\omega}_k \boldsymbol{\upsilon}_k^T \quad (21)$$

$$\mathbf{R}_{k+1} = (1-\gamma)\mathbf{R}_k + \gamma \boldsymbol{\upsilon}_k \boldsymbol{\upsilon}_k^T \tag{22}$$

with

$$\boldsymbol{\omega}_k = \frac{1}{T}(\hat{\boldsymbol{\theta}}_{k+1} - \hat{\boldsymbol{\theta}}_k) \tag{23}$$

$$\boldsymbol{\upsilon}_k = \mathbf{y}_{k+1} - \mathbf{h}\left(\mathbf{y}_k, \mathbf{u}_k, \hat{\boldsymbol{\theta}}_k\right) \tag{24}$$

For implementation, as well as the choice of suitable initial conditions for $\mathbf{Q}_0$, $\mathbf{R}_0$ and $\mathbf{S}_0$, two tuning parameters are now required, γ and λ. γ applies an exponentially weighted moving average to the propagation of the noise matrices in order to introduce an appropriate memory of the error history into the covariance. It can better be interpreted in terms of the filtering time constant, τ it introduces, by

$$\gamma = 1 - e^{-T/\tau} \tag{25}$$

λ performs a similar function to the design covariance $E\left(\boldsymbol{\omega}_k^{(\boldsymbol{\theta})} \boldsymbol{\omega}_k^{(\boldsymbol{\theta})T}\right)$, in [4]. Set in the range $0 < \lambda < 1$, it diminishes the expectation of error in the change in parameters, stabilising the identification. Put simply, the filter causes parameter adaptation which induces (a desirable) non-zero $\dot{\boldsymbol{\theta}}_k$. However, these changes are *errors* according to the zero model of eqn (13), and if their *total* magnitude is interpreted as error, $\mathbf{Q}_k$ becomes relatively large compared with $\mathbf{R}_k$, which results in an increase in the feedback gain $\mathbf{K}_k$ to provide greater correction to the $\boldsymbol{\theta}$. Subsequent parameter corrections are then larger, and this induces instability. λ provides a means of balancing the filter such that changes in $\mathbf{Q}_k$ are, correctly, not interpreted entirely as error.

Performance and stability studies on the setting of these parameters are given in [1] and [2], so these will not be elaborated further here. Essentially, $\mathbf{Q}_0$ and λ provide the principal means of influencing the speed of adaptation of the algorithm, τ can be nominally set according to the time history to be used for identification, $\mathbf{R}_0$ can be calculated directly from eqn (14), and $\mathbf{S}_0 = \mathbf{0}$ is appropriate (with $\mathbf{S}_0 \neq \mathbf{0}$ developing naturally as the IEKF runs).

3. THE IDENTIFIED MODEL

A 3DOF yaw-roll-sideslip model structure is adopted for identification, with fixed roll centres and with the roll axis parallel to the SAE *x* axis. The principle equations of motion are,

for sideslip,

$$M\dot{v} + Mhp\dot{} = \sum_{i=1,4} F_{yi} - Mur \tag{26}$$

for yaw,

$$I_{zz}\dot{r} = b\sum_{i=1,2} F_{yi} - c\sum_{i=3,4} F_{yi} \tag{27}$$

and for roll,

$$\begin{aligned} Mh\dot{v} + I_{xx}\dot{p} &= -Mhur - 2Bp + \left(Mgh - K_f - K_r\right)\phi \\ \dot{\phi} &= p \end{aligned} \tag{28}$$

Lateral load transfer is provided for by calculating vertical loads on the tyres using

$$\begin{aligned} F_{z1,2} &= \frac{cMg}{2(b+c)} \pm \frac{\left(F_{y1,2}h_f - K_f\phi - Bp\right)}{t_f} \\ F_{z3,4} &= \frac{bMg}{2(b+c)} \pm \frac{\left(F_{y3,4}h_r - K_r\phi - Bp\right)}{t_r} \end{aligned} \tag{29}$$

and the tyre slip angles are assumed equal on each axle, with a steering compliance compensation at the front :

$$\begin{aligned} \alpha_1 = \alpha_2 &= \left(\frac{-v - br}{u}\right) + \delta - \frac{\pi S \sum_{i=1,2} F_{yi}}{180Mg} \\ \alpha_3 = \alpha_4 &= \left(\frac{rc - v}{u}\right) \end{aligned} \tag{30}$$

The four load varying lateral tyre forces F_{yi} are then given by an adaptation of the Pacejka magic formula seen in [5], using slip normalisation such that :

$$C_\alpha = c_1 Mg\left(1 - e^{-\frac{c_2 F_z}{Mg}}\right), \quad F_p = \frac{F_z}{1 + \left(3F_z / 2Mg\right)^3} \tag{31}$$

$$\bar{\alpha} = \frac{GC_\alpha \alpha}{PF_p} \tag{32}$$

$$R = \sin\left(C\tan^{-1}\left(\bar{\alpha}/C - E\left(\bar{\alpha}/C - \tan^{-1}\left(\bar{\alpha}/C\right)\right)\right)\right) \tag{33}$$

$$F = PF_p R \tag{34}$$

The lateral forces then evolve from a necessary lag function which nominally accounts for slip transients in the tyre,

$$F_{y(k+1)} = \gamma_y F_{(k)} + \left(1 - \gamma_y\right) F_{y(k)} \tag{35}$$

The model is executed within the IEKF by establishing symbolic (Matlab Symbolic Math) descriptions of the state derivatives, and setting

$$\mathbf{y} = \begin{bmatrix} r \\ v \\ p \end{bmatrix}, \qquad \mathbf{h}_{k+1} = \mathbf{y}_k + T\dot{\mathbf{y}}_k \tag{36}$$

And to avoid excessively long expressions in the Jacobian, an intermediate symbolic variable *F* (eqn 34) is employed, with Jacobian components calculated using chain rule differentiation;

$$\frac{\partial h_m}{\partial \theta_n} = \frac{\partial h_m(F)}{\partial \theta_n} + \sum_i \frac{\partial h_m(F)}{\partial F_i}\frac{\partial F_i}{\partial \theta_n} \tag{37}$$

Table 1 summarises the model nomenclature and fixed parameter values, which were set where possible using manufacturer's data. Tyre data appropriate to the class of vehicle was obtained from [5] and Dixon [6].

Table 1 Model nomenclature and parameters

States, **x**	
r	Yaw angular velocity (*rad/s*)
v	Sideslip velocity (*m/s*)
p	Roll angular velocity (*rad/s*)
ϕ	Roll angle (*rad*)
Parameters, θ (*default values*)	
M	Mass (*1840 kg*)
I_{zz}	Yaw moment of inertia (*4140 kgm²*)
I_{xx}	Roll moment of inertia (*735 kgm²*)
b, c	CG to front / rear axle distance (wheelbase *3.03 m*)
h	CG height above roll axis
$h_{f/r}$	Height of front / rear roll centre (*0.1 m*)
$t_{f/r}$	Front / rear track (*1.56 m*)
$K_{f/r}$	Front / rear roll stiffness (*59 / 36 kNm/rad*)
B	Roll damping (front / rear equal) (*1225 Nms/rad*)
S	Steering compliance (*°/g acting at front axle*)
c_1,c_2	Tyre cornering stiffness coefficients (*3, 7*)
P	Tyre peak force (road friction) coefficient
G	Tyre cornering stiffness gain coefficient
C, E	Tyre model shape coefficients
γ_y	Tyre lag factor (*as eqn (25) with τ = 0.1*)
Inputs, **u**	
δ	front wheel steer angle (*rad*)
u	forward velocity (*m/s*)

4. VEHICLE TESTING AND TYRE MODEL

The test vehicle is a 2002my X350 3.5l Jaguar XJ8. An Oxford Technical Solutions RT3200 combined GPS / inertial measurement system was used to provide all the required data apart from the handwheel steer angle, which was sourced from the vehicle CAN. All data was collected and re-sampled where necessary at 100Hz to match the IEKF set with T = 0.01s.

Identification and validation drives were conducted on a flat, dry proving ground. The identification data comprises a sequence of step steer events, carried out at cruise controlled constant speed, with each event achieving a steady-state lateral acceleration for a few seconds before returning and again settling to zero steer. Steps with progressively higher magnitude were conducted up to and slightly beyond the terminal understeer condition (though the combination of rear-wheel drive and cruise control caused nearer neutral / oversteer limit behaviour on occasion, that was suitably controlled by the driver). The sequence was repeated at several fixed speeds. The validation data comprised a 'free drive' around the proving ground with low frequency randomly varying speed and steer manoeuvres.

Given the measurement of yaw and lateral accelerations along with all of the constituent variables required to formulate tyre slip angles, it is possible to construct a scatter plot of the normalised tyre behaviour directly from the measurements. This is not independent of an assumed tyre and vehicle model, but it does provide a useful measure of the consistency of the tyre behaviour and hence the feasibility of direct 'single model' tyre identification.

To generate the plot, cumulative axle force is deduced from measured lateral and yaw accelerations a_y and $\dot{r}$:

$$\begin{bmatrix} F_{yf} \\ F_{yr} \end{bmatrix} = \begin{bmatrix} 1 & 1 \\ b & -c \end{bmatrix}^{-1} \begin{bmatrix} Ma_y \\ I_{zz}\dot{r} \end{bmatrix} \tag{38}$$

An estimate of vehicle roll angle,

$$\hat{\phi} = \frac{-\left(F_{yf} + F_{yr}\right)h}{K_f + K_r + Mgh} \tag{39}$$

is then applied to eqn (29) to estimate the tyre vertical loads. (Measured roll angle suffers from low frequency errors since it is an absolute measure and small road camber angles are not insignificant and unknown.)

Measured δ, u, v and r are applied to eqns (30) – (32) to find F in order to attribute an appropriate left / right split to the 'measured' data F_{yf} and F_{yr}, and hence find an equivalent 'measured' R by inversion of eqn (34) :

$$R_1 = \left(\frac{F_1}{F_1 + F_2}\right)\frac{F_{yf}}{PF_p}, \quad R_2 = \left(\frac{F_2}{F_1 + F_2}\right)\frac{F_{yf}}{PF_p} \quad \text{etc} \tag{40}$$

The four measurement based R_i and $\overline{\alpha}_i$, plotted in Fig 1 show how the measurements on the identification drive emulate eqn (33). Alterations to parameter choices will obviously influence the plot, but it is clear both that the expected shape exists, and that the four corners provide consistent behaviour. Note however that direct optimisation of parameters from this plot cannot be achieved, since (eg) $P \to \infty$ or $G \to 0$ tend to a zero slip null solution. The IEKF objective is to match the model to each discrete update of the measured states, so it doesn't suffer such severe conditioning problems.

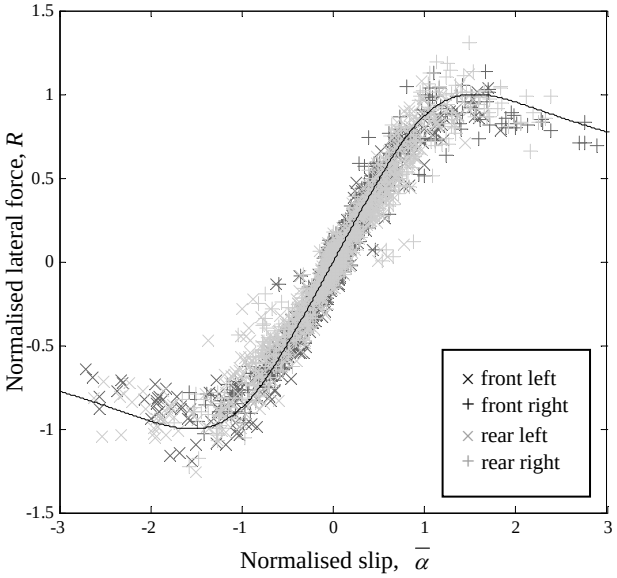

Fig. 1 Normalised tyre interpreted from vehicle test data

5. IEKF RESULT

Prior to application within the IEKF, the vehicle data is filtered in the frequency domain by zeroing frequencies above 6Hz using a DFT. This post-processing is not essential, and would clearly be omitted or replaced with suitable real-time filters in any on-line application of the IEKF, but it provides improvements in speed and consistency of the parameter convergence when the algorithm is used, as here, for system identification.

The experiment uses four step-steer sequences, at 13, 16, 21 and 24 m/s. The mid-range around 18m/s is avoided since at this speed, CG lateral velocities experience an anti-node. The aim is to optimise performance principally through identification of the 'single tyre', so the parameter set is

θ = [*P* (0.9), *G* (1), *C* (1.4), *E* (-0.2), *S* (2), *a* (1.5), *h* (0.5)]

where the bracketed numbers show the initial condition θ_0, which are 'best guess' approximations, using manufacturers data and tyre data resources [5] and [6].

Inclusion of *a* and *h* allow lateral and vertical optimisation of the CG, which guards against any mis-calibration of the CG position in the set-up of the instrumentation, ensuring that the (highly sensitive) lateral velocity, and (less critical) roll rate signals are correctly referenced.

The IEKF is run over the 360 seconds of data repeatedly, for several iterations, with its own sensitivity parameters set to promote slow and steady parameter optimisation. This is achieved by setting τ=350 (consistent with the test duration) and λ=0.01, $\mathbf{Q}_0=10^{-6}\mathbf{I}$ (for further guidance see [2]).

Fig. 2 shows the convergence for the first 20 iterations of the data, and Fig. 3 shows sections of data which typify the open loop performance of the final, converged parameter set, in comparison with θ_0; table 2 summarises RMS errors.

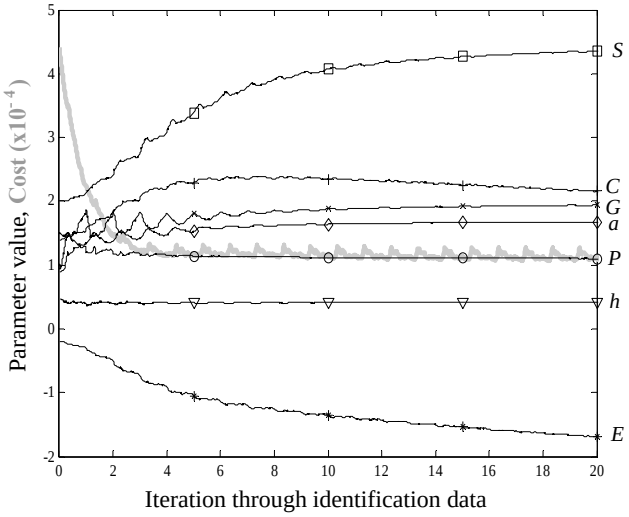

Fig. 2 Parameter and cost convergence

The optimised parameter set is

θ = [1.072, 1.956, 1.782, -2.291, 4.519, 1.689, 0.408]

which shows physically sensible results throughout; *S*=4.5 equates to just over 2°/g compliance.

Fig. 2 shows that trace($\mathbf{R}_k$) (the best measure of cost*, giving aggregated error in $\boldsymbol{y}_k$) decays rapidly over the first few iterations, and that four of the parameters converge equally quickly. The remaining, slower parameters are therefore relatively poorly conditioned within the set, but these do converge within 50 iterations. There is some indication that *E* may continue to fall if alternative sensitivity parameters are employed in the IEKF however. Fig. 1 was compiled using the optimised parameter set and this illustrates the

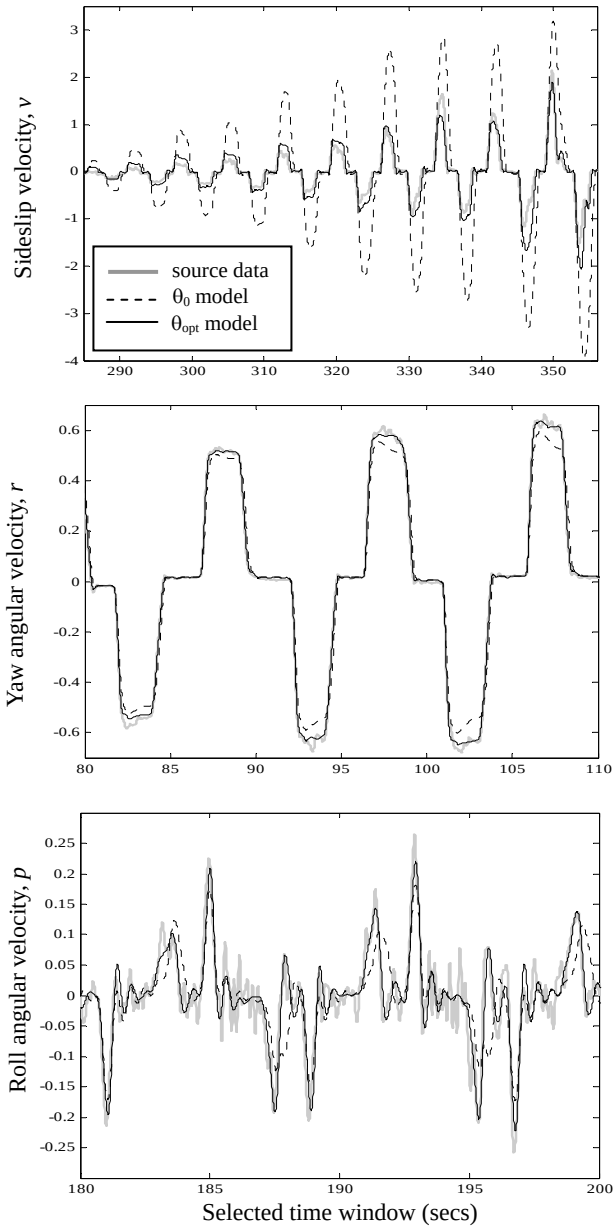

* The actual cost criterion of the IEKF is trace($\mathbf{P}_k$), but this gives *expectation* of parameter error, not actual performance.

Fig. 3 Identification data state time histories

identified tyre curve; we can see the influence of a low *E* setting which can ultimately turn the curve towards even lower *R* for high magnitude $\bar{\alpha}$ (creating a more distinct 'S' shape). If *E* is omitted from the optimisation, slightly poorer performance figures are returned, in exchange for a flatter tyre curve.

Table 2 State estimation performance

RMS error / RMS signal (%)						
		v	*r*	*p*	ϕ	a_y
Identification	θ_0	239	13	69	31	27
	θ_{opt}	45	5	52	13	9
Validation	θ_0	290	17	78	58	34
	θ_{opt}	66	7	54	45	11

Fig. 4 shows open-loop performance on the validation data, with a_y rather than *r* illustrated for variety – both yield very similar, excellent performance. In this section of the test, speed varies between 14 and 18 m/s, so the anti-node case is seen, where very low *v* predominates. Both Fig. 3(a) and Fig. 2(a) show an excellent improvement in tracking *v*, which is clearly attributable to the identified tyre model. The phase correction and improved prediction of *p* is also impressive.

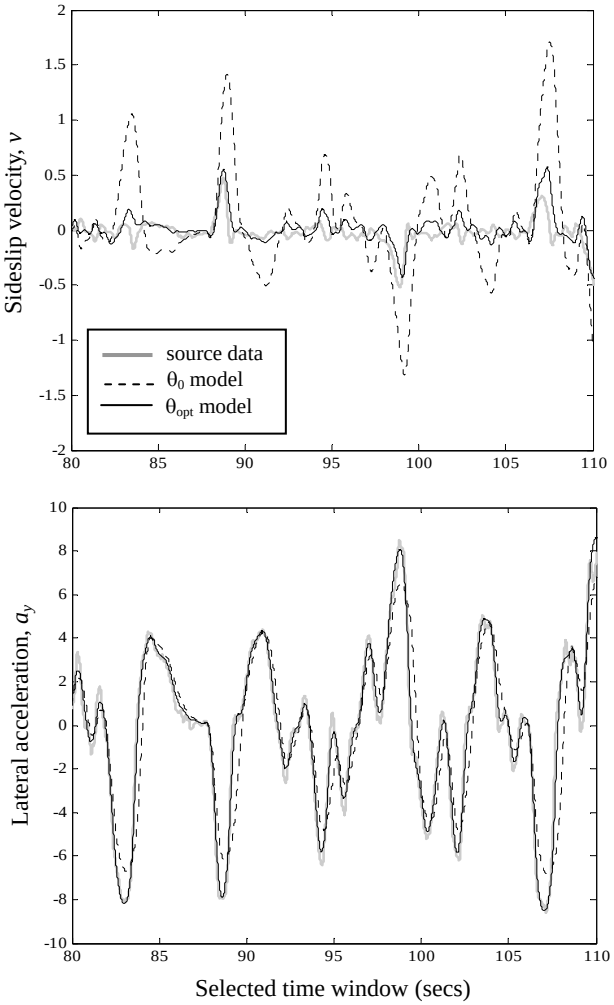

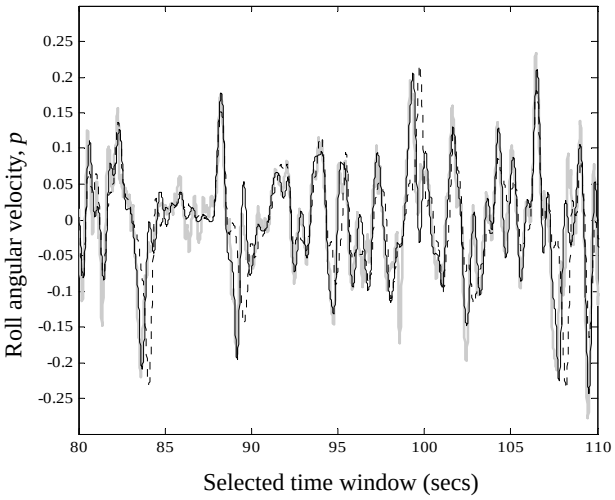

Fig. 4 Validation data time histories

6. CONCLUSION

Results using the initial parameter set, θ_0 show that reasonably accurate parameters allow the simple model structure used here to provide good estimation of yaw rate and lateral acceleration. However we see that a sub-optimal tyre model prevents correct lateral velocity and hence tyre slip prediction. The IEKF solution shows that excellent performance, including correct tyre slip prediction, can be gained from the simple model structure. Moreover it is also clear that the method allows a simple, single tyre model to be successfully identified directly from the vehicle test data.

REFERENCES

[1]. Best, M.C., "Parametric identification of vehicle handling using an extended Kalman filter", International Journal of Vehicle Autonomous Systems, Vol 5, No 3 / 4, 2007, pp 256 – 273.

[2]. Best, M.C., Newton, A.P. and Tuplin, S, "The identifying extended Kalman filter: parametric system identification of a vehicle handling model", Proc. Instn Mech. Engrs, Part K: J. Multi-body Dynamics, 2007, 221(O1), 87-98.

[3]. Bolzern, P., Cheli., F., Falciola, G. and Resta, F., "Estimation of the Non-Linear Suspension Tyre Cornering Forces from Experimental Road Test Data", Vehicle System Dynamics, 1999, vol 31 no 1, pp 23-34.

[4]. Best M.C., Gordon T.J. and Dixon P.J., "An Extended Adaptive Kalman Filter for Real-time State Estimation of Vehicle Handling Dynamics", Vehicle System Dynamics, 2000, vol 34, no 1, pp 57-75.

[5]. Milliken W.F. and Milliken D.L. (1995), "Race Car Vehicle Dynamics", SAE International.

[6]. Dixon J.C. (1996), "Tires, Suspension and Handling", SAE International.